Article

Synthesis, Antifungal Activity, Cytotoxicity and QSAR Study of Camphor Derivatives

Xinying Duan [1,†], Li Zhang [1,†], Hongyan Si [1], Jie Song [2], Peng Wang [1], Shangxing Chen [1], Hai Luo [1], Xiaoping Rao [3], Zongde Wang [1,*] and Shengliang Liao [1,*]

[1] East China Woody Fragrance and Flavor Engineering Research Center of National Forestry and Grassland Administration, Camphor Engineering Research Center of National Forestry and Grassland Administration, College of Forestry, Jiangxi Agricultural University, Nanchang 330045, China; duan19990226@163.com (X.D.); zhangli_miaomuli@163.com (L.Z.); hongyansi16@163.com (H.S.); pengwang1981@126.com (P.W.); csxing@126.com (S.C.); luohai87@126.com (H.L.)

[2] Department of Natural Sciences, University of Michigan-Flint, 303E Kearsley, Flint, MI 48502, USA; jiesong@umich.edu

[3] College of Chemical Engineering, Huaqiao University, Xiamen 361021, China; rxping2001@163.com

[*] Correspondence: zongdewang@163.com (Z.W.); liaosl@jxau.edu.cn (S.L.); Tel.: +86-0791-83813243 (S.L.)

[†] These authors contributed equally to this work.

Abstract: Control of fungal phytopathogens affecting crops and woodlands is an important goal in environmental management and the maintenance of food security. This work describes the synthesis of 37 camphor derivatives, of which 27 were new compounds. Their antifungal effects on six fungi were evaluated in vitro. Compounds **3a**, **4a** and **5k** showed strong antifungal activity against *Trametes versicolor*, with EC_{50} values of 0.43, 6.80 and 4.86 mg/L, respectively, which were better than that of tricyclazole (EC_{50} 118.20 mg/L) and close to or better than that of carbendazim (EC_{50} 1.20 mg/L). The most potent compound, **3a**, exhibited broad-spectrum antifungal activity towards six fungi with EC_{50} values within the range of 0.43–40.18 mg/L. Scanning electron microscopy demonstrated that compounds **3a**, **4a** and **5k** gave irregular growth and shriveling of the mycelia. In vitro cytotoxicity evaluation revealed that the tested camphor derivatives had mild or no cytotoxicity for LO_2 and HEK293T cell lines. Quantitative structure−activity relationship (QSAR) analysis revealed that the number of F atoms, relative molecular weight, the atomic orbital electronic population and total charge on the positively charged surfaces of the molecules of camphor derivatives have effects on antifungal activity. The present study may provide a theoretical basis for a high-value use of camphor and could be helpful for the development of novel potential antifungals.

Keywords: camphor; synthesis; antifungal activity; cytotoxicity; QSAR

1. Introduction

In modern agriculture, phytopathogenic fungi not only severely reduce grain yield and quality, but also secrete toxins that endanger the health of humans and animals [1]. In addition, wood rot fungi can seriously degrade wood products [2]. At present, the chemical fungicides widely used to control phytopathogenic and wood rot fungi are economical, easy to use and efficient. However, the misuse of chemical fungicides can result in the rapid development of resistance and serious environmental contamination [3,4]. The development of novel highly efficient, low-toxicity and ecofriendly alternative fungicides is urgently needed. Preparation of novel antifungals from plant essential oils and some of their main components has attracted attention because of their broad-spectrum antifungal properties, mechanisms of action and environmental compatibility [5–12].

The naturally occurring monoterpenketone camphor is found in *Cinnamomum camphor*, and it can also be obtained by the isomerization–oxidation of turpentine. Due to its biological activity and variable molecular structure, camphor has potential as a building

block in the preparation of biologically active derivatives [13–16]. The development of camphor-based anti-microbial derivatives has recently been reported [17–22]. For example, Ma et al. [21] synthesized novel camphoric-acid-based acylhydrazone derivatives, with some of the most active compounds giving growth inhibition of 90.00%-95.00% at 0.05 mg/mL. Such results suggest the feasibility of developing novel anti-microbial agents with camphor as a raw material.

Thiosemicarbazides (TSCs) have attracted much attention because they can impart antifungal properties on compounds [23,24]. For instance, Qin et al. [25] synthesized novel thiosemicarbazone chitosan derivatives and demonstrated these compounds exhibited broad-spectrum antifungal activity against four common crop-threatening pathogenic fungi. Furthermore, Yamaguchi et al. found that TSC–camphene derivatives had excellent antifungal effects on *Trichophyton menthagophytes* through damage to the fungal cell wall. The MIC value of the most active antifungal compound was 55.00 µmol L^{-1} [26]. The potential antifungal activity of camphor and TSCs focused our efforts on the development of some novel TSC–camphor derivatives as antifungal candidates.

Herein, two series of camphor derivatives have been designed, synthesized and characterized. Their antifungal effects on *Phytophthora nicotianae*, *Fusarium verticillioides*, *Colletotrichum gloeosporioides*, *Sphaeropsis sapinea*, *Fusarium oxysporum* and *Trametes versicolor* were assessed. The in vitro cytotoxicity of representative camphor derivatives were evaluated on LO$_2$ and HEK293T. The morphological changes in camphor derivatives against *T. versicolor* were assessed using scanning electron microscopy (SEM). Quantitative structure–activity relationship (QSAR) analysis was used to detect the relationships between structural features and antifungal effects on *T. versicolor*. The current study may provide a theoretical basis for the high-value utilization of camphor, and could help the development of novel potential antifungals against phytopathogenic and wood rot fungi.

2. Materials and Methods

2.1. Materials and Equipment

Camphor, thiosemicarbazide, bromobenzyl derivatives, *α*-bromoacetophenone derivatives, carbendazim and tricyclazole were purchased from Shanghai Aladdin Reagent Co., Ltd. (Shanghai, China). Ethanol, isopropanol, acetonitrile, petroleum ether, dimethyl sulfoxide and ethyl acetate were purchased from Xilong Science Co., Ltd. (Guangdong, China). Potato dextrose agar (PDA) were purchased from Huan Kai Microbial Technology Co., Ltd. (Guangdong, China). Melting points were determined with the WRS-2 melting point apparatus (Shanghai Precision and Scientific Instrument Co., Ltd., Shanghai, China) and were uncorrected. FT-IR analysis was performed on the Nicolet iS50 Fourier Transform Infrared Spectrometer (Thermo, Waltham, MA, USA). The ^{1}H NMR and ^{13}C NMR spectra were measured on an AVANCE 400 spectrometer (Thermo, Waltham, MA, USA) using CDCl$_3$ or DMSO-d_6 as the solvent. High-resolution mass spectrometry (HRMS) spectra were recorded on a triple time of flight TOF 5600+ (AB Sciex) mass spectrometer (Concord, ON, Canada). Cytotoxicity data was measured by microplate reader Tecan Infinite 200 Pro (Tecan Trading AG, Maennedorf, Switzerland) at 492 nm. The mycelium morphologies of *T. versicolor* were observed using a scanning electron microscope (Hitachi, Regulus 8100, Tokyo, Japan).

Five phytopathogenic fungi, namely *Phytophthora nicotianae* (*P. nicotianae*), *Fusarium verticillioides* (*F. verticillioides*), *Colletotrichum gloeosporioides* (*C. gloeosporioides*), *Sphaeropsis sapinea* (*S. sapinea*) and *Fusarium oxysporum* (*F. oxysporum*) were isolated and identified by the plant pathology laboratory at the College of Agriculture, Jiangxi Agricultural University. The wood rot fungus *Trametes versicolor* cfcc5336 was purchased from China Forestry Culture Collection Center. All strains and incubated in PDA at 26 °C.

2.2. Synthesis of Camphor Derivatives

2.2.1. Synthesis of 2-(1,7,7-Trimethylbicyclo [2.2.1]heptan-2-ylidene)hydrazine-1-carbothio amide (**3a**)

Camphor (10 mmol) and thiosemicarbazide (10 mmol) were dissolved in a round-bottom flask (50 mL) containing isopropanol (20 mL) and 10% HCl (1 mL). The mixture was stirred for 4 h at room temperature. The progress of the reaction was checked by thin-layer chromatography (TLC) with the developing solvent ethyl acetate/petroleum ether (4.5:1, V/V). The precipitates were collected by vacuum filtration in a fume hood, and the filtered cake was washed with petroleum ether. The solid powder was recrystallized with ethanol and H_2O, filtered under vacuum, washed with petroleum ether (3 × 100 mL) and dried in an oven to obtain the white solid compound **3a**. The synthetic routes to compound **3a** and its derivatives are shown in Figure 1. Compound **3a** was characterized by ^{1}H NMR, ^{13}C NMR, FT-IR and HRMS (Supplementary Materials Figures S1, S36, S71 and S106).

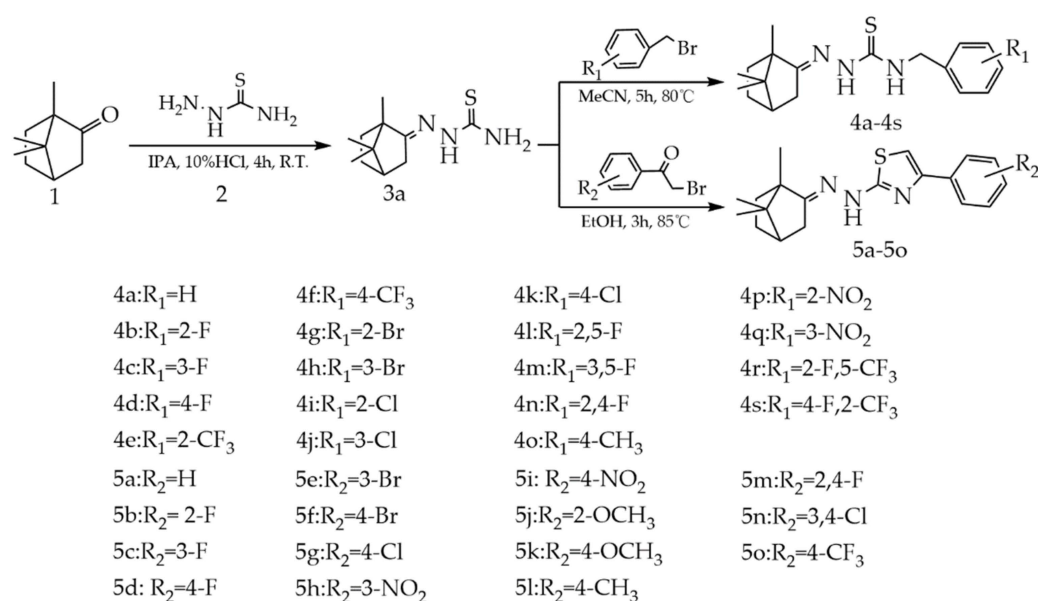| 4a:R_1=H	4f:R_1=4-CF_3	4k:R_1=4-Cl	4p:R_1=2-NO_2
4b:R_1=2-F	4g:R_1=2-Br	4l:R_1=2,5-F	4q:R_1=3-NO_2
4c:R_1=3-F	4h:R_1=3-Br	4m:R_1=3,5-F	4r:R_1=2-F,5-CF_3
4d:R_1=4-F	4i:R_1=2-Cl	4n:R_1=2,4-F	4s:R_1=4-F,2-CF_3
4e:R_1=2-CF_3	4j:R_1=3-Cl	4o:R_1=4-CH_3	
5a:R_2=H	5e:R_2=3-Br	5i: R_2=4-NO_2	5m:R_2=2,4-F
5b:R_2= 2-F	5f:R_2=4-Br	5j:R_2=2-OCH_3	5n:R_2=3,4-Cl
5c:R_2=3-F	5g:R_2=4-Cl	5k:R_2=4-OCH_3	5o:R_2=4-CF_3
5d: R_2=4-F	5h:R_2=3-NO_2	5l:R_2=4-CH_3	

Figure 1. Synthetic routes of camphor derivatives.

2.2.2. Synthesis of N-(2-Chlorobenzyl)-2-(1,7,7-trimethylbicyclo[2.2.1]heptan-2-ylidene)hyd razine-1-carbothioamide compounds (**4a–4s**)

Substituted benzyl bromide (12 mmol) was added dropwise over 30 min to a stirred solution of compound **3a** (10 mmol) in acetonitrile (20 mL) that was stirred and heated to 80 °C, for 5 h. After the reaction was complete, solids precipitated on the bottom of the round-bottom flask. The precipitates were collected through vacuum filtration in a fume hood, and the filtered cake was washed with petroleum ether. The solid powder was recrystallized with ethanol and H_2O, filtered under vacuum, washed with petroleum ether (3 × 100 mL) and dried in an oven to give the pure product (**4a–4s**). The synthetic routes to compound **4a–4s** are shown in Figure 1. Compound **4a–4s** were characterized by ^{1}H NMR, ^{13}C NMR, FT-IR and HRMS (Supplementary Materials Figures S2–S20, S37–S55, S72–S90, and S107–S125).

2.2.3. Synthesis of 4-Phenyl-2-(2-(1,7,7-trimethylbicyclo[2.2.1]heptan-2-ylidene)hydrazinyl) thiazole compounds (**5a–5o**)

A stirred solution of compound **3a** (10 mmol) in ethanol (50 mL) was added to α-bromoacetophenone derivatives (10 mmol) in a round-bottom flask (100 mL). The mixture was stirred and heated to 85 °C, for approximately 3 h, evaporated under reduced pressure to remove the organic phase, and the solid powder was collected by vacuum filtration in a fume hood. Then, the solid powder was recrystallized with ethanol, filtered under vacuum, washed with petroleum ether (3×100 mL) and dried in an oven to give the pure product

(**5a**–**5o**). The synthetic routes to compound **5a**–**5o** are shown in Figure 1. Compound **5a**–**5o** were characterized by ^{1}H NMR, ^{13}C NMR, FT-IR and HRMS (Supplementary Materials Figures S21–S35, S56–S70, S91–S105 and S126–S140).

2.3. In Vitro Antifungal Activity Evaluation

The in vitro antifungal activity of the camphor derivatives against six fungi was evaluated using the mycelium growth rate method [27], with the commercial fungicides tricyclazole and carbendazim serving as positive controls. Dimethyl sulfoxide was used as a carrier control. The camphor derivatives dissolved in dimethyl sulfoxide to generate stock solutions (1.0×10^4 mg/L), which were further diluted to 250, 125, 62.5, 31.3, 15.6, 7.81, 3.91, 1.95, 0.977, 0.488 and 0.244 mg/L, respectively, in PDA plates. Mycelial disks (0.50 cm) of activated fungi were added to PDA plates and incubated at 26 °C for 4–7 days. All tests were repeated three separate experiments. The Cross method was used to measure the colony diameter in the Petri dishes of treatment groups, once the colony diameter reached approximately 68–72 mm in the Petri dish of the untreated control. The inhibition rate (IR) reflected the antifungal activity of each compound and was calculated as Equation (1):

$$IR(\%) = (B - T)/(B - 0.5) \text{ (cm)} \times 100\% \tag{1}$$

where B and T are the diameters of the blank control and treatment groups, respectively. The effective concentration giving 50% inhibition (EC_{50}) for each of the tested compounds was analyzed by probit analysis within the SPSS statistics software.

2.4. Cytotoxicity (MTT) Assays

The 3-(4, 5-dimethylthiazolyl-2)-2,5-diphenyltetrazolium bromide (MTT) assay was used to assess the in vitro cytotoxicity of the compounds on two human cell lines, LO_2 and HEK293T [28]. The LO_2 and HEK293T were cultured in Dulbecco's modified eagle medium (DMEM). In the tested group, the cell lines were treated with 10 mg/L of the compounds for 24 h in 96-well plates, and cell lines treated without compounds were used as the blank control. After 24 h treatment, 20 µL MTT solution (5 mg/mL) was added to each well, followed by 4 h incubation. Finally, the absorbance of the wells at 492 nm was measured using a microplate reader Tecan Infinite 200 Pro. The experiment was repeated three times. Cell viability was evaluated as the ratio of the absorbance of antifungal treated to untreated cells.

2.5. Scanning Electron Microscope (SEM) Observations

Freshly cultured mycelia were inoculated on PDA plates containing no compound, compounds **3a**, **4a**, or **5k** and incubated at 26 °C, for 7 days, placed on a glass slide and dehydrated [29]. The morphology of the mycelia was observed by SEM.

2.6. Quantitative Structure−Activity Relationship (QSAR) Study

The structure of each of the synthesized compounds was drawn using Gauss view 5.0.9 software (Gaussian, Inc. Wallingford, CT, USA). The density functional theory (DFT) method at the B3LYP 6-31G(d) level of Gaussian 09W (Gaussian, Inc. Wallingford, CT, USA) [30] was used to optimize the molecular structures and calculate the minimum energy of the camphor derivatives. Then, Ampac 8.16 software (Semichem, Inc. Shawnee, KS, USA) [31] was used to convert the Gaussian 09W output files into Ampac output files, which were compatible with Codessa 2.7.10 software (Semichem, Inc. Shawnee, KS, USA) [32]. Twenty-nine camphor derivatives were selected and assigned to the modeling dataset, and the remaining camphor derivatives (compounds **4q**, **4i**, **4j**, **4l**, **5i**) were randomly selected for assignment to the external validation dataset. $Log_{50}EC_{50}$ of the camphor derivatives was taken as the dependent variable of the QSAR model equation, while the molecular structure descriptors of camphor derivatives provided the independent variables of the QSAR model. Regression analysis of the molecular structures and antifungal activity was carried out using the heuristic method encoded in Codessa 2.7.10 software [33], and the quantitative

relationship models were constructed. The best QSAR model was determined by the "breaking point" criterion ($\Delta R^2 < 0.02$–0.04) [34]. Finally, "leave-one-out" cross-validation, internal validation and external validation were used to validate the QSAR model.

3. Results and Discussion

3.1. Chemistry

The synthesis of **3a**, **5a**, **5d**, **5f**, **5g**, **5i**, **5k** and **5l** was first reported by Sokolova et al. [35]. Here, two series of 35 camphor derivatives were synthesized, of which 27 were new compounds. In Sokolova's study [35], via catalysis using sulfuric acid, compound **3a** was prepared by reacting camphor with thiosemicarbazide for 10 h, with a yield of 74.00%. In the present study, hydrochloric acid was used as catalyst instead of sulfuric acid, the reaction time was shortened to 4 h, and the yield of compound **3a** was increased to 93.24 % (Supplementary Materials Page 4).

Compounds **4a**–**4s** were produced via the reaction between compound **3a** and benzyl bromide or substituted benzyl bromide, at 80 °C, for 5 h (Figure 1). The progress of the reaction was monitored by TLC. All the products were purified by recrystallization. The yields of compounds **4a**–**4s** reached 78.15~87.22% (Supplementary Materials Page 4–14). This synthetic route had the advantage of a short reaction time, fewer by-products and simple post-treatment method.

Compounds **5a**–**5o** were synthesized via the reaction between compound **3a** and α-bromoacetophenone or substituted α-bromoacetophenone, at 85 °C, for 3 h (Figure 1), with ethanol used as a solvent. The yields of the products reached 49.98~92.11% (Supplementary Materials Page 14–21). In Sokolova's study [35], N-Bromosuccinimide and p-toluenesulfonic acid were used as catalysts, with a mixture of ethanol and $CHCl_3$ used as a solvent; the reaction was carried out for 24 h, and the product yield was 34.00~71.00%. In the present work, the reaction conditions were optimized, no catalyst was used, the solvent was simplified to ethanol, the reaction temperature was increased to 85 °C, and the products were more efficiently prepared, with ideal yields. The products were characterized by ^{1}H NMR, ^{13}C NMR, FT-IR and HRMS. The structural characterization data indicated that compounds **3a**, **4a**–**4s** and **5a**–**5o** were successfully synthesized (Supplementary Materials Figures S1–S140).

3.2. In Vitro Antifungal Activity and Structure−Activity Relationship (SAR)

The antifungal activity of camphor derivatives was tested against *P. nicotianae*, *F. verticillioides*, *C. gloeosporioides*, *S. sapinea*, *F. oxysporum* and *T. versicolor*. The commercial fungicides tricyclazole and carbendazim were used as positive controls. The results showed the camphor derivatives exhibited antifungal activity against six fungi to various extents (Figure 2, Table 1, Supplementary Materials Table S1–S6). *T. versicolor* was the most sensitive organism to the camphor derivatives compared with the other five fungi. Camphor and thiosemicarbazone had a weak inhibitory effect on six fungi. Compounds **3a** and **4a**–**4s** displayed low to medium activity, with EC_{50} values ranging from 25.08 to >1000 mg/mL against *P. nicotianae*, 31.32 to >1000 mg/mL against *F. verticillioides*, 12.85 to >1000 mg/mL against *C. gloeosporioides*, 17.09 to >1000 mg/mL against *S. sapinea* and 15.89 to >1000 mg/mL against *F. oxysporum*. Compounds **5a**–**5o** showed almost no antifungal activity against these five fungi.

However, the camphor derivatives (**3a**, **4a**–**4s** and **5a**–**5o**) exhibited moderate to potent antifungal activity against *T. versicolor*. Of these compounds **3a**, **4a**, **4d**, **4o**, **5a**, **5g**, **5k** and **5l** showed potent antifungal activity against *T. versicolor*, with EC_{50} values of 0.43, 6.80, 7.67, 6.89, 4.42, 7.85, 4.86 and 5.09 mg/L, respectively, which were superior to the values obtained for tricyclazole (EC_{50} 118.20 mg/L, Supplementary Materials Figure S142 and Table S6) and comparable to or better than those for carbendazim (EC_{50} 1.20 mg/L, Supplementary Materials Figure S143 and Table S7). At 15.6 mg/L, the inhibition by compounds **3a**, **4a**, **4d**, **4o**, **5a**, **5g**, **5k** and **5l** against *T. versicolor* was >50.00% (Supplementary Materials Table S6). Notably, compound **3a** displayed broad-spectrum antifungal activity; its EC_{50} values

against six fungi were 25.10, 40.18, 12.85, 17.09, 19.30 and 0.43 mg/L, respectively (Table 1 and Figure 2). It exhibited a stronger antifungal effect on six fungi than the positive control tricyclazole (EC_{50}: 80.58, 185.93, 79.39, 268.37, 66.78 and 118.20 mg/L, respectively). Even at 0.244 mg/L, the inhibition by compound **3a** against *T. versicolor* was >33.20% (Figure 2, Supplementary Materials Table S6).

Table 1. EC_{50} values of camphor-based derivatives against six fungi [a].

Compd.	EC_{50} (mg/L)					
	PN	**FV**	**CG**	**SS**	**FO**	**TV**
1	>1000	>1000	>1000	>1000	597.01	>1000
2	215.66	172.24	92.44	159.50	118.14	150.55
3a	25.08	40.18	12.85	17.09	19.30	0.43
4a	207.80	82.34	36.51	93.51	38.56	6.80
4b	253.14	88.85	34.94	109.93	15.89	99.70
4c	176.72	63.91	28.91	86.14	16.24	35.78
4d	158.81	69.10	30.62	101.23	19.97	7.67
4e	89.92	62.16	80.49	100.08	20.05	593.17
4f	>1000	>1000	74.00	>1000	734.52	361.20
4g	>1000	>1000	771.99	>1000	>1000	>1000
4h	79.78	34.39	65.66	69.47	29.85	101.99
4i	>1000	45.97	330.96	>1000	899.39	>1000
4j	101.81	39.68	26.90	54.04	38.55	68.47
4k	91.87	40.54	24.09	77.58	21.03	17.18
4l	178.16	58.83	59.23	120.53	20.80	204.45
4m	137.26	31.32	34.65	/	25.05	107.66
4n	174.28	66.43	35.03	127.07	16.33	342.56
4o	>1000	206.14	136.85	>1000	42.63	6.89
4p	341.97	131.69	33.22	162.35	38.88	18.86
4q	>1000	>1000	52.24	>1000	730.69	51.49
4r	73.59	645.97	80.55	101.04	26.50	>1000
4s	112.39	723.36	82.85	76.73	56.45	>1000
5a	>1000	125.46	371.75	>1000	>1000	4.42
5b	>1000	>1000	364.55	>1000	486.83	11.30
5c	>1000	816.15	639.90	>1000	>1000	7.40
5d	>1000	>1000	769.85	>1000	>1000	40.93
5e	>1000	>1000	522.47	>1000	>1000	139.57
5f	>1000	>1000	>1000	>1000	>1000	101.56
5g	>1000	>1000	652.17	>1000	>1000	7.85
5h	>1000	>1000	233.73	>1000	>1000	12.37
5i	>1000	>1000	>1000	>1000	/	/
5j	>1000	>1000	474.68	>1000	>1000	16.24
5k	>1000	>1000	489.08	>1000	>1000	4.86
5l	>1000	>1000	33.64	>1000	>1000	5.09
5m	>1000	>1000	>1000	>1000	/	294.86
5n	>1000	>1000	>1000	>1000	>1000	>1000
5o	>1000	>1000	634.710	>1000	/	>1000
tricyclazole	80.58	185.93	79.39	268.37	66.78	118.20
carbendazim	1.49	0.55	0.20	4.67	0.45	1.20

Note: [a] PN, *Phytophthora nicotianae*; FV, *Fusarium verticillioides*; CG, *Colletotrichum gloeosporioides*; SS, *Sphaeropsis sapinea*; FO, *Fusarium oxysporum*; TV, *Trametes versicolor*. "/" means no antifungal activity.

T. versicolor is a common polypore species found throughout the world. It grows easily under different types of environment and is a suitable model organism for screening new antifungal agents. In the present study, camphor derivatives had good antifungal activity against *T. versicolor* and more modest activity against another five phytopathogenic fungi, indicating that camphor derivatives could serve as leading compounds in the discovery of novel broad-spectrum antifungal agents.
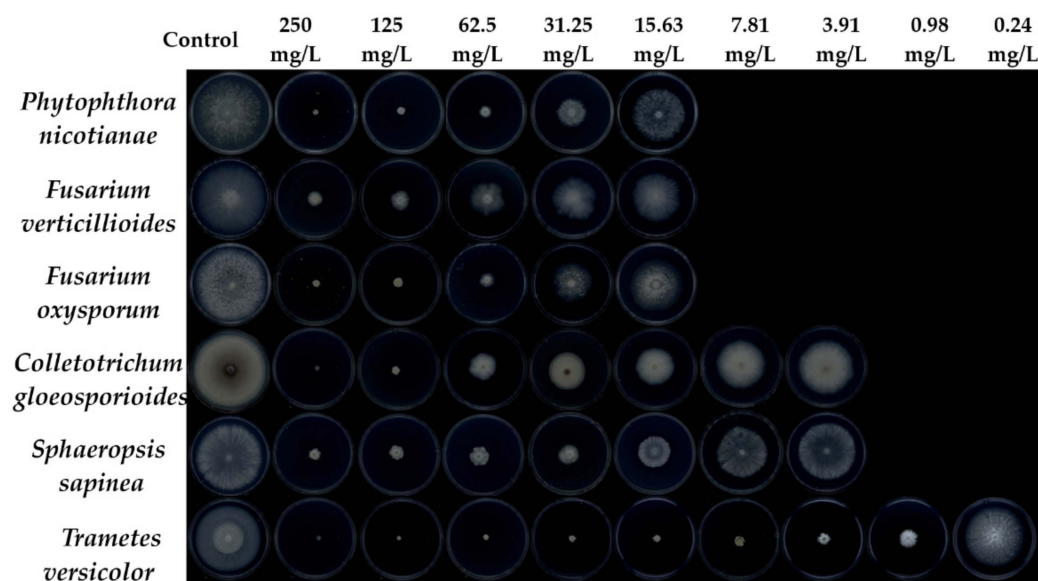
Figure 2. Photographs of antifungal experiments of compound **3a** against six fungi.

Previous studies have reported that thiosemicarbazide (TSC) is a multi-target compound that can affect the cell cycle regulation of fungi and inhibit the metabolism of various nutrients [36]. Hence, it has been widely used in the preparation of fungicides, such as Thiophanate-Methyl [37]. In the present study, the thiosemicarbazide group was fused with the camphor backbone, in order to obtain derivatives with good activity against fungi. As anticipated, compound **3a**, the product formed by the reaction of thiosemicarbazide and camphor, exhibited much better antifungal activity than thiosemicarbazide and camphor. This result indicated that fusion of the thiosemicarbazide group and the camphor skeleton greatly enhanced the antifungal activity of the derivative.

Some broad conclusions can be drawn from analysis of structure–activity relationships of camphor derivatives against *T. versicolor*. Most of the compounds, namely, **4a–4s** and **5a–5o**, exhibited better antifungal activity against *T. versicolor* compared with camphor and thiosemicarbazone. A comparison of the effects of the substituents on the benzene ring on antifungal activity against *T. versicolor* showed compounds **4a** (EC$_{50}$ 6.80 mg/L) and **5a** (EC$_{50}$ 4.42 mg/L), with no substituents in the benzene ring, displayed better antifungal activity than the other derivatives **4b–4s** and **5b–5o**. The introduction of additional electron-withdrawing or electron-donating groups on the benzene ring did not enhance the antifungal activity of the derivatives against *T. versicolor*. When the same substituent groups were introduced into the benzene ring of the derivatives, the number of substituent groups had improved the antifungal activity against *T. versicolor* [38]. It was found that derivatives monosubstituted with fluorine exerted stronger antifungal activity than those polysubstituted with fluorine (**4b–4d** > **4l–4n**; **5b–5d** > **5m**) corroborating of prior research [39]. The analysis of the effect of substituent position in the benzene ring on antifungal activity against *T. versicolor* showed that derivatives with a substituent group at the para-position generally gave better antifungal activity (**4d** > **4b**, **4c**; **4k** > **4i**, **4j**; **5k** > **5j**, etc.).

3.3. Evaluation of Cytotoxicity

Fourteen camphor derivatives (**1**, **3a**, **4a**, **4d**, **4p**, **5a–5d**, **5g**, **5h** and **5j–5l**) with good antifungal activity against *T. versicolor* were evaluate for cytotoxicity on two human cell lines, LO$_2$ and HEK293T, using the MTT assay (Figure 3). All the tested compounds exhibited mild to no cytotoxicity for LO$_2$ and HEK293T cells at a concentration of 10 mg/L. Figure 3c,d show that the LO$_2$ and HEK293T cells treated by the tested derivatives remained healthy and round. Among the tested compounds, the raw material camphor was found to be non-toxic for LO$_2$ and HEK293T cells. The intermediate compound 3a, with the best antifungal activity against *T. versicolor,* showed mild cytotoxicity towards LO$_2$ and

HEK293T cells (proportional cell viability> 90% at 10 mg/L, Figure 3a,b). The other camphor derivatives were not toxic towards LO_2 and HEK293T cells.
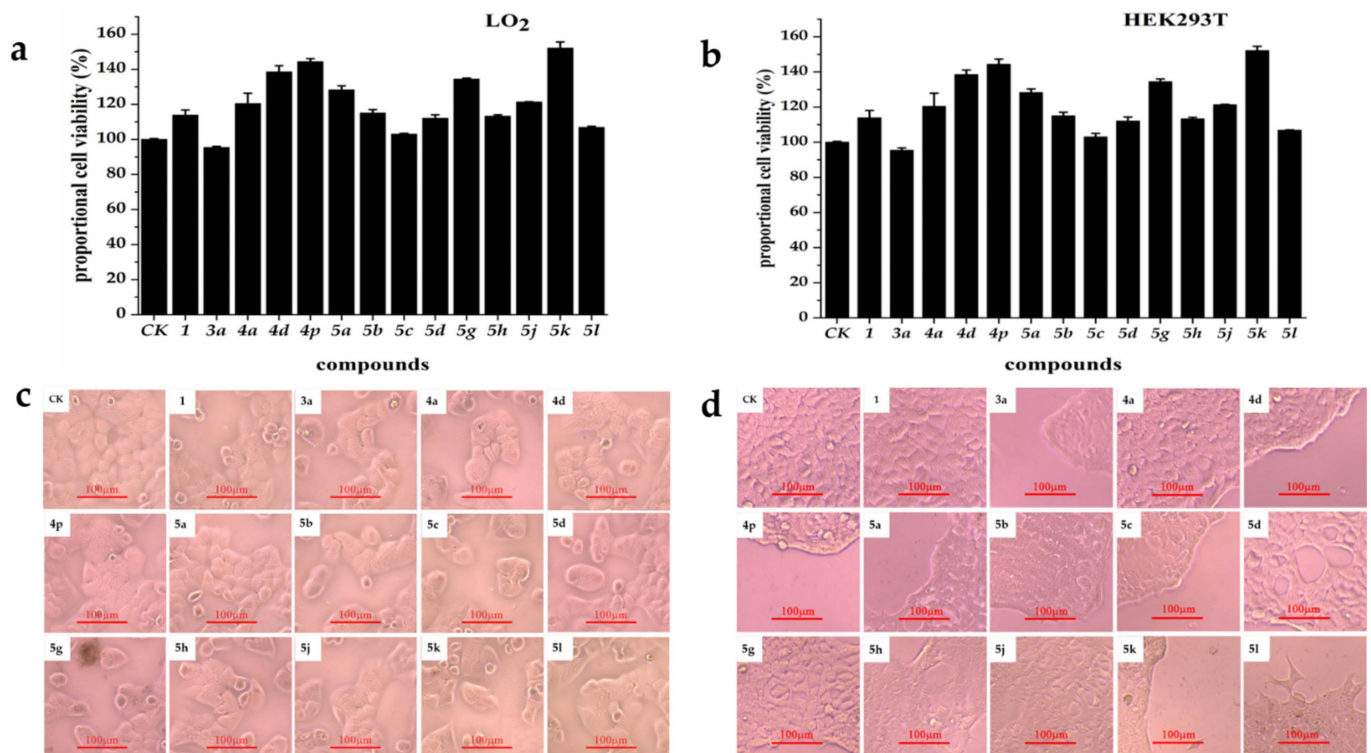

Figure 3. In vitro cytotoxicity of several camphor derivatives: (**a**) proportional viability of LO_2 cells in response to 10 mg/L of compound; (**b**) proportional viability of HEK293T cells in response to 10 mg/L of compound; (**c**) photographic image of LO_2 cells in response to 10 mg/L of compound; (**d**) photographic image of HEK293T cells in response to 10 mg/L of compound.

LO_2 and HEK293T represent cells normally found in human liver and kidney, respectively, where they are important cells for metabolism. Since pesticides may be ingested during use, it was important to evaluate the toxicity of pesticides on such cells. Our results show the camphor derivatives synthesized in present study have low toxicity or are non-toxic for LO_2 and HEK293T cells. These results suggest that these camphor derivatives may be promising lead compounds in the development of low-toxicity antifungals.

3.4. Effect on the Mycelium Morphology of T. versicolor

Compounds **3a**, **4a** and **5k**, with excellent antifungal activity against *T. versicolor*, were evaluated for their effects on the morphology of *T. versicolor*. The ultrastructural of *T. versicolor* mycelia treated with compounds **3a**, **4a** and **5k** and a reagent blank control were observed by SEM. The results in Figures 4 and S141 show that the surface of *T. versicolor* mycelium treated with compounds **3a**, **4a** and **5k** become folded and shriveled (Figure 4b–d). In contrast, the hyphae of the untreated control group showed a smooth surface and normal growth (Figure 4a). Together with previous research findings [40,41], we speculate that the fungal cell walls and cell membranes of *T. versicolor* are potential targets of the camphor derivatives, but the mechanism of action of camphor derivatives needs further study.
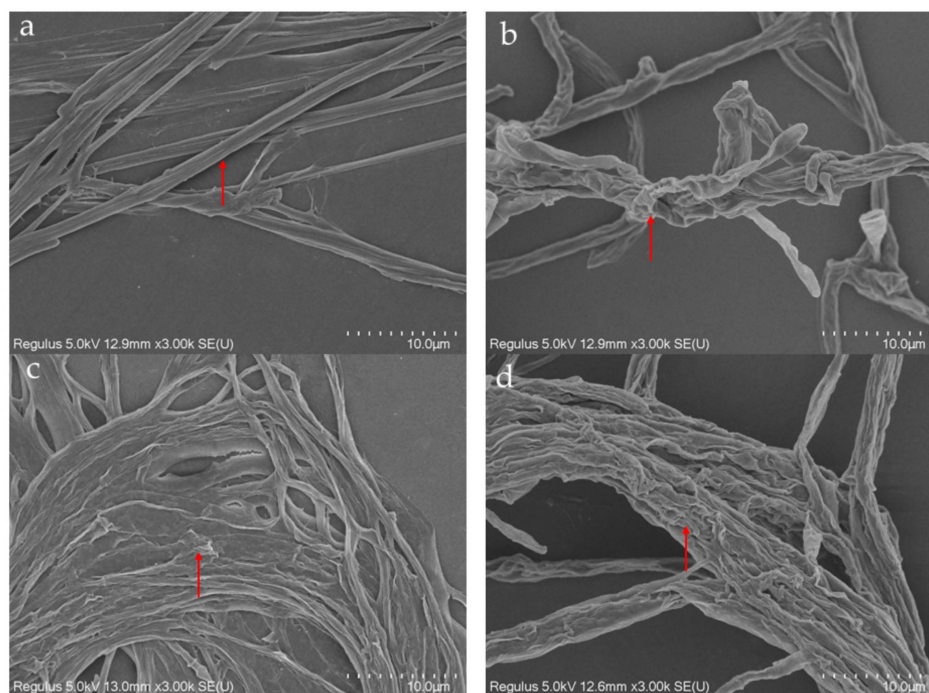
Figure 4. Scanning electron micrographs of mycelial morphology of *T. versicolor*: (**a**) blank control, ×3000; (**b**) treated with compound **3a** at 0.43 mg/L (EC$_{50}$), ×3000; (**c**) treated with compound **4a** at 6.80 mg/L (EC$_{50}$), ×3000; (**d**) treated with compound **5k** at 4.86 mg/L (EC$_{50}$), ×3000. The red arrows point out the healthy mycelium and the damaged mycelium.

3.5. QSAR Study

A QSAR analysis was carried out to identify quantitative relationship between the molecular structures of the camphor derivatives and their antifungal activity against *T. versicolor*. A series of QSAR models with different numbers of descriptors were obtained using the heuristic method encoded in Codessa 2.7.10. According to the "breaking point" criterion, the best QSAR model, which contained four descriptors (R^2 = 0.911, F = 61.5, s^2 = 0.0973), was obtained through linear regression analysis (Figure 5a). The details of the model are listed in Table 2, and a comparison of experimental and calculated log$_{50}$ EC$_{50}$ values is shown in Figure 5b. The figure shows a strong correlation resulting in only small differences between the experimental log$_{50}$ EC$_{50}$ values and the calculated log$_{50}$ EC$_{50}$ values, thus indicating that the best QSAR model is satisfactory.
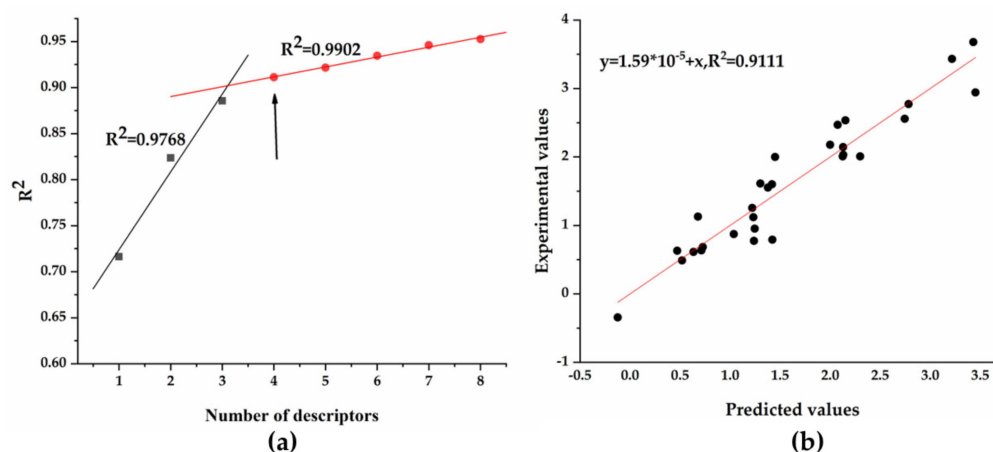

Figure 5. Confirmation of the number of descriptors and prediction of antifungal activity against *T. versicolor* using model constructed. (**a**) Application of the "breaking point" rule; (**b**) experimental and predicted log$_{50}$ EC$_{50}$ values.

**Table 2.** Details of the four-descriptor QSAR model.

Descriptor No.	Regression Coefficient (X)	Standard Error (ΔX)	*t*-Test	Descriptors
0	1.757	1.904	0.922	Intercept
1	0.416	0.052	8.067	NOF [a]
2	0.903	0.1008	8.960	RMW [b]
3	−11.104	2.862	−3.880	MAOEP [c]
4	0.528	0.203	2.578	FPSA-2 [d]

Note: [a] Number of F atoms; [b] Relative molecular weight; [c] Minimum atomic orbital electronic population; [d] FPSA-2 Fractional PPSA (PPSA-2/TMSA) [Quantum-Chemical PC].

In order to verify the robustness of the best QSAR model, "leave-one-out" cross-validation and internal validation were carried out, and the results are shown in Table 3. There was an acceptable difference between the squared correlation coefficients R^2 (0.911), R_{loo}^2 (0.844), $R_{training}^2$ (0.894) and R_{test}^2 (0.880) of the best QSAR model, indicating that the QSAR model was robust. In addition, the predictability of the best QSAR model was validated by external validation, and the results are illustrated in Figure 6. The squared correlation coefficient of external validation $R_{external}^2$ was 0.654, confirming that the prediction ability of the best QSAR model was satisfactory.

Table 3. Internal validation of QSAR model.

R^2	R_{loo}^2	Training Set	N	R^2 (Fit)	Test Set	N	R^2 (Fit)
0.911	0.844	A + B	20	0.924	C	9	0.886
		B + C	19	0.886	A	10	0.831
		A + C	19	0.882	B	10	0.922
		Average	-	0.897	Average	-	0.880
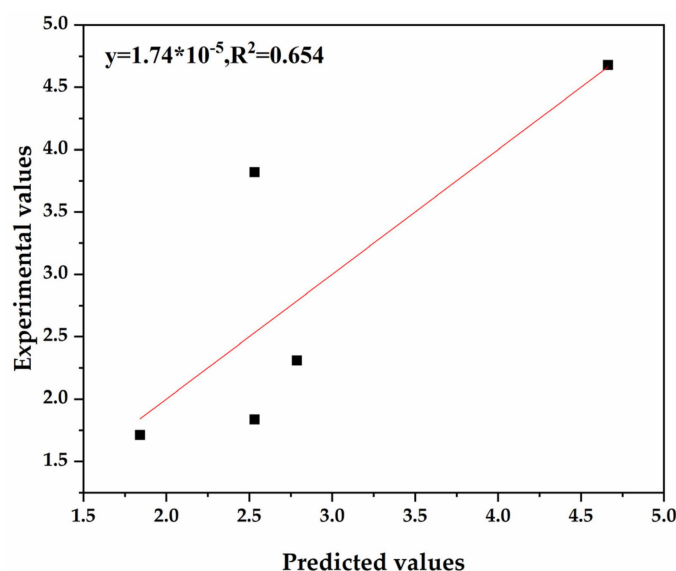
Figure 6. Comparison of the experimental values $\log_{50} EC_{50}$ and predicted values $\log_{50} EC_{50}$ based on external validation.

Based on the data listed in Table 2, the best QSAR model can be written as a linear regression equation:

$$\log_{50} EC_{50} = 1.757 + 0.416 \times NO + 0.903 \times RMW - 11.104 \times MAOEP + 0.528 \times FPSA\text{-}2$$
$$N = 29, R^2 = 0.911, F = 61.5, s^2 = 0.0973$$

(2)

N represents the number of camphor derivatives in the modeling dataset, R^2 represents the squared value of the correlation coefficient of the model, F represents the Fisher test value, and s^2 represents the variance of the model. Moreover, because the result of the t-test was positively correlated with the importance of the descriptors, it could be determined that the *Relative molecular weight* and *Number of F atoms* were the two most important descriptors affecting the antifungal activity of the camphor derivatives against *T. versicolor*.

According to Codessa's Reference Manual [42,43], the descriptors used to construct the best QSAR model can be explained as follows.

The first descriptor was *Number of F atoms*, which is classified as a constitutional descriptor. This descriptor was positively related to the $\log_{50} EC_{50}$ value of the camphor derivatives, i.e., it was negatively related to the antifungal activity of the camphor derivatives against *T. versicolor*. A previous study had shown that the introduction of F atoms could increase drug permeability across the cell membrane and allow small-molecule compounds to penetrate the fungal cell membrane more easily, a feature that can strongly affect the antifungal activity of compounds [44]. Based on the SAR and QSAR of the present study, although fluorine atoms improved the antifungal activity of the camphor derivatives, greater numbers of fluorine atoms did not necessarily increase the antifungal activity of the camphor derivatives. Interestingly, a previous study drew similar conclusions [39].

The second most important descriptor was *Relative molecular weight*, which is also a constitutional descriptor. This descriptor was negatively related to the antifungal activity of the camphor derivatives. Generally, a low molecular weight most effectively improve the efficient binding between target proteins with compound receptors [45]. Our in vitro antifungal activity study found that the compounds **3a**, **4a** and **5a**, with lower molecular mass, showed better antifungal activity. These results suggest that molecular weight is an important parameter to be considered when designing novel camphor derivatives.

The third descriptor, *Minimum atomic orbital electronic population*, belongs to the family of quantum-chemical descriptors. It is a charge-distribution-related descriptor connected with the orbital electronic population [33]. It is a vital physical parameter that describes the nucleophilicity of compounds [46] that could affect the interaction between camphor derivatives and their targets. In the best QSAR model, this descriptor was the sole descriptor with a positive contribution to the antifungal activity of the camphor derivatives. We speculated that a lower value for minimum atomic orbital electronic population helped improve the antifungal activity of the camphor derivatives.

The fourth descriptor was *FPSA-2 Fractional PPSA (PPSA-2/TMSA) [Quantum-Chemical PC]*, which is an electrostatic descriptor [47]. This descriptor describes the total number of charges contained on the positively charged surface of a molecule and is closely related to molecular charge distribution and shape. This descriptor negatively correlated with the antifungal activity of the camphor derivatives. It showed that a lower total charge number on the positively charged surface of a molecule improved the antifungal activity of camphor derivatives.

In summary, the QSAR analysis revealed that fewer fluorine atoms, a lower relative molecular weight, a lower value for minimum atomic orbital electronic population, and a lower total charge on the positively charged surface of the molecule helped improve the antifungal activity of the camphor derivatives against *T. versicolor*.

4. Conclusions

Two series of camphor derivatives were successfully and efficiently synthesized in this work. Bioassays showed that the camphor derivatives **3a**, **4a** and **5k** showed potent antifungal activity against *T. versicolor* and low toxicity against two human cell lines, LO_2 and HEK293T, suggesting that they may be promising lead compounds for the development of low-toxicity antifungals. SEM analysis showed that the camphor derivatives can markedly change the mycelial morphology of *T. versicolor*. In addition, SAR and QSAR studies provide useful information for the further design of camphor derivatives with improved antifungal activity. These findings lay a foundation and provided a reference for

the development of camphor derivatives as novel antifungals. However, the mechanism of action of camphor derivatives has yet to be determined, and research on this aspect will be carried out in a further study.

References

1. Salvatore, M.M.; Andolfi, A. Phytopathogenic Fungi and Toxicity. *Toxins* **2021**, *13*, 689. [CrossRef] [PubMed]
2. Wu, C.-C.; Huang, S.-L.; Ko, C.-H.; Chang, H.-T. Antifungal Sesquiterpenoids from *Michelia formosana* Leaf Essential Oil against Wood-Rotting Fungi. *Molecules* **2022**, *27*, 2136. [CrossRef] [PubMed]
3. El-Baky, N.A.; Amara, A.A.A.F. Recent Approaches towards Control of Fungal Diseases in Plants: An Updated Review. *J. Fungi* **2021**, *7*, 900. [CrossRef] [PubMed]
4. Price, C.; Parker, J.; Warrilow, A.; Kelly, D.E.; Kelly, S.L. Azole fungicides—Understanding resistance mechanisms in agricultural fungal pathogens. *Pest Manag. Sci.* **2015**, *71*, 1054–1058. [CrossRef]
5. Nazzaro, F.; Fratianni, F.; Coppola, R.; De Feo, V. Essential Oils and Antifungal Activity. *Pharmaceuticals* **2017**, *10*, 86. [CrossRef]
6. Wang, H.; Yang, Z.; Ying, G.; Yang, M.; Nian, Y.; Wei, F.; Kong, W. Antifungal evaluation of plant essential oils and their major components against toxigenic fungi. *Ind. Crop. Prod.* **2018**, *120*, 180–186. [CrossRef]
7. Amini, J.; Farhang, V.; Javadi, T.; Nazemi, J. Antifungal Effect of Plant Essential Oils on Controlling Phytophthora Species. *Plant Pathol. J.* **2016**, *32*, 16–24. [CrossRef]
8. Xie, Y.; Wang, Z.; Huang, Q.; Zhang, D. Antifungal activity of several essential oils and major components against wood-rot fungi. *Ind. Crop. Prod.* **2017**, *108*, 278–285. [CrossRef]
9. Broda, M. Natural Compounds for Wood Protection against Fungi—A Review. *Molecules* **2020**, *25*, 3538. [CrossRef]
10. Deepa, N.; Achar, P.N.; Sreenivasa, M.Y. Current Perspectives of Biocontrol Agents for Management of *Fusarium verticillioides* and Its Fumonisin in Cereals—A Review. *J. Fungi* **2021**, *7*, 776. [CrossRef]
11. Gao, Y.; Tian, X.; Li, J.; Shang, S.; Song, Z.; Shen, M. Study on Amphipathic Modification and QSAR of Volatile Turpentine Analogues as Value-Added Botanical Fungicides against Crop-Threatening Pathogenic Fungi. *ACS Sustain. Chem. Eng.* **2016**, *4*, 2741–2747. [CrossRef]
12. Guo, Y.Y.; Chen, J.B.; Ren, D.; Du, B.D.; Wu, L.; Zhang, Y.Y.; Wang, Z.Y.; Qian, S. Synthesis of osthol-based botanical fungicides and their antifungal application in crop protection. *Bioorg. Med. Chem.* **2021**, *40*, 116184. [CrossRef]
13. Kong, W.; Huo, H.; Gu, Y.; Cao, Y.Q.; Wang, J.L.; Liang, J.Y.; Niu, S.Q. Antifungal activity of camphor against four phyto-pathogens of Fusarium. *S. Afr. J. Bot.* **2022**, *148*, 437–445. [CrossRef]
14. Mokbel, A.A.; Alharbi, A.A. Antifungal effects of basil and camphor essential oils against Aspergillus flavus and A. parasiticus. *Aust. J. Crop. Sci.* **2015**, *9*, 532–537.
15. Gazdağlı, A.; Sefer, Ö.; Yörük, E.; Varol, G.I.; Teker, T.; Albayrak, G. Investigation of camphor effects on Fusarium graminearum and F. culmorum at different molecular levels. *Pathogens* **2018**, *7*, 90. [CrossRef]
16. Mahilrajan, S.; Nandakumar, J.; Kailayalingam, R.; Manoharan, N.A.; SriVijeindran, S. Screening the antifungal activity of essential oils against decay fungi from palmyrah leaf handicrafts. *Biol. Res.* **2014**, *47*, 1–5. [CrossRef]

17. Shokova, E.A.; Kim, J.K.; Kovalev, V. Camphor and its derivatives. Unusual transformations and biological activity. *Russ. J. Org. Chem.* **2016**, *52*, 459–488. [CrossRef]

18. Anjaneyulu, B.; Sangeeta; Saini, N. A Study on Camphor Derivatives and Its Applications: A Mini-Review. *Curr. Org. Chem.* **2021**, *25*, 1404–1428. [CrossRef]

19. Petkova, Z.; Valcheva, V.; Momekov, G.; Petrov, P.; Dimitrov, V.; Doytchinova, I.; Stavrakov, G.; Stoyanova, M. Antimyco-bacterial activity of chiral aminoalcohols with camphane scaffold. *Eur. J. Med. Chem.* **2014**, *81*, 150–157. [CrossRef]

20. Huang, Y.; Duan, W.G.; Lin, G.S.; Cen, B.; Wang, F.; Lei, F.H. Syntheses and Biological Activities of Camphor-Based Benzamide Compounds. *Chem. Bull.* **2014**, *9*, 878–882. (In Chinese)

21. Ma, X.-L.; Li, F.; Duan, W.-G.; Liao, J.-N.; Lin, Z.-D.; Lin, G.-S.; Cen, B.; Lei, F.-H. Synthesis and antifungal activity of camphoric acid-based acylhydrazone compounds. *Holzforschung* **2014**, *68*, 889–895. [CrossRef]

22. Abo-Bakr, A.M.; Hassan, E.A.; Mahdy, A.H.S.; Zayed, S.E. Synthetic and biological studies on some new camphor thiazoli-dinones. *J. Iran. Chem. Soc.* **2021**, *4128*, 2757–2769. [CrossRef]

23. Altalhi, A.A.; Hashem, H.E.; Negm, N.A.; Mohamed, E.A.; Azmy, E.M. Synthesis, characterization, computational study, and screening of novel 1-phenyl-4-(2-phenylacetyl)-thiosemicarbazide derivatives for their antioxidant and antimicrobial activities. *J. Mol. Liq.* **2021**, *333*, 115977. [CrossRef]

24. Nevagi, R.J.; Dhake, A.S.; Narkhede, H.I.; Kaur, P. Design, synthesis and biological evaluation of novel thiosemicarbazide analogues as potent anticonvulsant agents. *Bioorganic Chem.* **2014**, *54*, 68–72. [CrossRef]

25. Qin, Y.K.; Xing, R.; Liu, S.; Li, K.C.; Meng, X.T.; Li, R.F.; Cui, J.H.; Li, B.; Li, P.C. Novel thiosemicarbazone chitosan derivatives: Preparation, characterization, and antifungal activity. *Carbohydr. Polym.* **2012**, *87*, 2664–2670. [CrossRef]

26. Yamaguchi, M.U.; Barbosada, S.A.; Ueda-Nakamura, T.; Dias, F.B.; Conceicaoda, S.C.; Nakamura, C.V. Effects of a thio-semicarbazide camphene derivative on Trichophyton mentagrophytes. *Molecules* **2009**, *14*, 1796–1807. [CrossRef]

27. Mao, S.; Wu, C.; Gao, Y.; Hao, J.; He, X.; Tao, P.; Li, J.; Shang, S.; Song, Z.; Song, J. Pine Rosin as a Valuable Natural Resource in the Synthesis of Fungicide Candidates for Controlling *Fusarium oxysporum* on Cucumber. *J. Agric. Food Chem.* **2021**, *69*, 6475–6484. [CrossRef]

28. Chao, Z.; Wu, J.; Reinhart-King, C.A.; Chu, C.C. Synthesis, characterization and cytotoxicity of photo-crosslinked maleic chitosan-polyethylene glycol diacrylate hybrid hydrogels. *Acta Biomater.* **2010**, *6*, 3908–3918.

29. Wang, W.; Cheng, X.; Cui, X.; Xia, D.G.; Wang, Z.Q.; Lv, X.H. Synthesis and biological activity of novel Pyrazolo [3,4-d]pyrimidin-4-one derivatives as potent antifungal agent. *Pest. Manag. Sci.* **2021**, *77*, 3529–3537. [CrossRef] [PubMed]

30. Frisch, M.J.; Trucks, G.W.; Schlegel, H.B.; Scuseria, G.E.; Robb, M.A.; Cheeseman, J.R.; Scalmani, G.; Barone, V.; Mennucci, B.; Petersson, G.A.; et al. *Gaussian 09*; Gaussian, Inc.: Wallingford, CT, USA, 2009.

31. Dewar, M.J.S.; Holder, A.J.; Dennington, R.D.; Liotard, D.A.; Truhlar, D.G.; Keith, T.A.; Millam, J.M.; Harris, C.D. *AMPAC 8 User Manual*; Semichem, Inc.: Shawnee, KS, USA, 2004.

32. Katritsky, A.; Karelson, M.; Lobanov, V.S.; Dennington, R.; Keith, T. *CODESSA 2.7.10.*; Semichem, Inc.: Shawnee, KS, USA, 2004.

33. Katritzky, A.R.; Dobchev, D.A.; Tulp, I.; Karelson, M.; Carlson, D.A. QSAR study of mosquito repellents using Codessa Pro. *Bioorganic Med. Chem. Lett.* **2006**, *16*, 2306–2311. [CrossRef] [PubMed]

34. Tämm, K.; Fara, D.C.; Katritzky, A.R.; Burk, A.P.; Karelson, M. A Quantitative Structure−Property Relationship Study of Lithium Cation Basicities. *J. Phys. Chem. A* **2004**, *108*, 4812–4818. [CrossRef]

35. Sokolova, A.S.; Yarovaya, O.L.; Bormotov, N.L.; Shishkina, L.N.; Salakhutdinov, N.F. Synthesis and antiviral activity of camphor-based 1,3-thiazolidin-4-one and thiazole derivatives as orthopoxvirus-reproduction inhibitors. *RSC Med. Chem.* **2018**, *9*, 1746–1753. [CrossRef]

36. Borba, J.V.V.B.; Tauhata, S.B.F.; Oliveira, C.M.A.D.; Marques, M.F.; Bailao, A.M.; Soares, C.M.D.A. Chemoproteomic identification of molecular targets of antifungal prototypes, thiosemicarbazide and a camphene derivative of thiosemicarbazide, in paracoccidioides brasiliensis. *PLoS ONE* **2018**, *13*, e0201948. [CrossRef]

37. De Mello, F.E.; Lopes-Caitar, V.S.; Prudente, H.; Xavier-Valencio, S.A.; Franzenburg, S.; Mehl, A.; Marcelino-Guimaraes, F.C.; Verreet, J.-A.; Balbi-Peña, M.I.; Godoy, C.V. Sensitivity of Cercospora spp. from soybean to quinone outside inhibitors and methyl benzimidazole carbamate fungicides in Brazil. *Trop. Plant Pathol.* **2021**, *46*, 69–80. [CrossRef]

38. Chen, Y.; Mi, Y.; Sun, X.; Zhang, J.; Li, Q.; Ji, N.; Guo, Z. Novel Inulin Derivatives Modified with Schiff Bases: Synthesis, Characterization, and Antifungal Activity. *Polymers* **2019**, *11*, 998. [CrossRef]

39. Pan, T.; Geng, Y.X.; Hao, J.; He, X.H.; Li, J.; Gao, Y.Q.; Shang, S.B.; Song, Z.Q. Taking advantage of the renewable forest bio-resource turpentine to prepare α,β- unsaturated compounds as highly efficient fungicidal candidates. *J. Agric. Food. Chem.* **2021**, *69*, 12985–12993. [CrossRef]

40. Zhang, L.; Shi, Y.; Duan, X.; He, W.; Si, H.; Wang, P.; Chen, S.; Luo, H.; Rao, X.; Wang, Z.; et al. Novel Citral-thiazolyl Hydrazine Derivatives as Promising Antifungal Agents against Phytopathogenic Fungi. *J. Agric. Food Chem.* **2021**, *69*, 14512–14519. [CrossRef]

41. Zhang, L.; Feng, X.Z.; Xiao, Z.Q.; Fan, G.R.; Chen, S.X.; Liao, S.L.; Luo, H.; Wang, Z.D. Design, Synthesis, Antibacterial, An-tifungal and Anticancer Evaluations of Novel β-Pinene Quaternary Ammonium Salts. *Int. J. Mol. Sci.* **2021**, *22*, 11299. [CrossRef]

42. Katritzky, A.R.; Lobanov, V.; Karelson, M. *CODESSA: Reference Manual*; University of Florida: Gainesville, FL, USA, 1994.

43. Katritzky, A.R.; Petrukhin, R.; Yang, H.; Karelson, M. *CODESSA PRO User's manual (Comprehensive Descriptors for Structural and Statistical Analysis)*; University of Florida: Gainesville, FL, USA, 2002.

44. Johnson, B.M.; Shu, Y.-Z.; Zhuo, X.; Meanwell, N.A. Metabolic and Pharmaceutical Aspects of Fluorinated Compounds. *J. Med. Chem.* **2020**, *63*, 6315–6386. [CrossRef]

45. Li, Q.; Kang, C.B. Mechanisms of action for small molecules revealed by structural biology in drug discovery. *Int. J. Mol. Sci.* **2020**, *21*, 5262. [CrossRef]

46. Girgis, A.S.; Saleh, D.O.; George, R.F.; Srour, A.M.; Pillai, G.G.; Panda, C.S.; Katritzky, A.R. Synthesis, bioassay, and QSAR study of bronchodilatory active 4H-pyrano [3,2-c]pyridine-3-carbonitriles. *Eur. J. Med. Chem.* **2015**, *89*, 835–843. [CrossRef]

47. Holder, A.J.; Ye, L.; Yourtee, D.M.; Agarwal, A.; Eick, J.D.; Chappelow, C.C. An application of the QM-QSAR method to predict and rationalize lipophilicity of simple monomers. *Dent. Mater.* **2005**, *21*, 591–598. [CrossRef]